

A Closed-Form Model for Image-Based Distant Lighting

Mais Alnasser and Hassan Foroosh

Abstract

In this paper, we present a new mathematical foundation for image-based lighting. Using a simple manipulation of the local coordinate system, we derive a closed-form solution to the light integral equation under distant environment illumination. We derive our solution for different BRDF's such as lambertian and Phong-like. The method is free of noise, and provides the possibility of using the full spectrum of frequencies captured by images taken from the environment. This allows for the color of the rendered object to be toned according to the color of the light in the environment. Experimental results also show that one can gain an order of magnitude or higher in rendering time compared to Monte Carlo quadrature methods and spherical harmonics.

Index Terms

Image-Based Relighting, Distant Light Modeling, Light Integral Equation, Lambertian and Phong models

I. INTRODUCTION

Image-based rendering (IBR) has been an active area of research in computational imaging and computational photography in the past two decades. It has led to many interesting non-traditional problems in image processing and computer vision, which in turn have benefited from traditional methods such as shape and scene description [1]–[3], [10], [11], [15], [16], [34], [36]–[38], [54], [56], [69]–[72], [75]–[78], [83], [85], [95], [101], [132], [134], [135], [137], [146], scene content modeling [79], [80], [84], [86]–[88], [139]–[143], super-resolution (in particular in 3D) [31]–[33], [46], [67], [68], [94], [104]–[106], [108]–[114], [117], [118], [120], video content modeling [9], [12]–[14], [17], [18], [35], [121]–[126], [133], [136], image alignment [6], [19]–[21], [23]–[26], [29], [30], [57]–[62], [64], [65], [107], [115], [116], tracking and object pose estimation [97]–[99], [119], [129], and camera motion quantification and calibration [8], [27], [39]–[41], [41]–[43], [45], [49]–[51], [63], [73], [74], [81], [82], [89]–[92], [96], to name a few.

Using images to estimate or model environment light for relighting objects introduced or rendered in a scene is a central problem in this area [4], [5], [22], [28], [44], [47], [48], [66], [100], [127], [144], [145]. This requires solving the light integral equation (also known as the rendering equation), which plays a crucial role in IBR. One of the oldest and most straightforward approaches for solving the integral is to approximate the solution using the Monte Carlo method [93]. However, Monte Carlo is an estimation method, and unless sufficient light samples are taken, it produces noisy results. Therefore, a substantial number of samples and accordingly more time is typically required in order to render a realistic low-noise image.

The key idea that we propose in this paper is the fact that any light source can be modeled as an area light source. For instance, a spot light or a directional linear light can both be modeled as special cases of an area light source, where the dimensionality has reduced. Similarly, environment lighting using cubemaps may be viewed as the limiting case of pointwise varying multiple area light sources. Therefore, in this paper, we first show how the light integral can be solved in closed-form for a constant area light source of rectangular shape. We apply our solution to rendering lambertian and Phong-like materials. We then extend our solution to non-constant pointwise varying light sources and apply our solution to lambertian surfaces. In order to streamline the understanding of the implementation issues, we also provide a pseudocode for our algorithm.

Because of the closed-form nature of our solution, no sampling is required and noise is completely eliminated. On the other hand, the lack of requirement for sampling reduces the rendering time significantly, making it dependent only on the complexity of the object (i.e. the number of triangles used to represent it) for a constant area light source, and dependent on the required highest light frequency in the case of pointwise varying environment lighting. In particular, in the case of low-frequency environment lighting, we achieve the same level of accuracy as spherical harmonics with coefficients reduced by an order of magnitude in $O(1)$ complexity. A very simple preprocessing of the light is required, to compress it using discrete cosine transform, which also happens to be the most classical tool for image compression.

II. RELATED WORK

Some very interesting closed-form solutions have already been proposed to solve the light integral. The appeal of closed-form solutions lies in the fact that they provide complete elimination of noise. Furthermore, the availability of a closed-form solution expedites the rendering process significantly. For estimation methods such as Monte Carlo [128], many samples of the

Mais Alnasser was with the Department of Computer Science, University of Central Florida, Orlando, FL, 32816 USA at the time this project was conducted. (e-mail: nasserm@cs.ucf.edu).

Hassan Foroosh is with the Department of Computer Science, University of Central Florida, Orlando, FL, 32816 USA (e-mail: foroosh@cs.ucf.edu).

environment are required to render realistic low-noise images. On the other hand, several hours might be required to generate one single image.

Currently, the closed-form solutions proposed in the literature mostly target specific scenarios. For example, the work done in [102] targets linear light sources and provides a solution to the integral for diffuse and specular materials lit by such a light. The work done by Arvo [7] provides analytic solutions to the light integral for polyhedral sources using the irradiance jacobian. [130] introduced the use of B-splines to represent surface radiance in static scenes. A recent work by Sun et al [131] provides a closed-form solution to the light integral given isotropic point light sources. Their solution targets the scenarios of fog, mist and haze.

Closed-form solutions were also proposed for special cases of non-constant lighting such as the work done by [52], which provides a solution for linearly-varying luminaires. The most common application for non-constant lighting is in environment maps. [103] used spherical harmonics to solve the light integral for diffuse materials lit by environment maps, and achieved real-time rendering.

The methods used to solve the light integral vary and so do the scenarios for which the light integral is solved. In addition to advantages described in the previous section in terms of compression and speed, one of our contributions is to provide a unified framework that works for spot light, area, and natural distant environment lighting. We achieve this by formulating a new closed-form solution to the lighting integral. Our framework works for lambertian and Phong-like materials. Mirrored, transmissive and textured materials can be easily embedded within the framework. We were able to achieve a constant complexity for lambertian materials depending only on the resolution of the rendered image, suggesting real-time if implemented on hardware.

III. SOLVING THE LIGHT INTEGRAL

Figure 1 shows the relationship between the incident light and the light leaving the surface of an object at a given point. The following is the the most general form of the light integral describing this relationship:

$$L_o(p, w_o) = L_e(p, w_o) + \int_{H(N)} f(p, w_o, A_i) L_i(p, A_i) \max(0, \cos \theta_i) \frac{\cos \theta_A}{r^2} dA_i \quad (1)$$

where w_o is the outgoing direction, $L_e(p, w_o)$ is the emitted light at point p in the direction w_o , $L_o(p, w_o)$ is the radiance leaving the surface at a point p in the direction w_o , $f(p, w_o, A_i)$ is the Bidirectional Reflectance Distribution Function (BRDF), $L_i(p, A_i)$ is the incident radiance emitted from the area patch A_i , θ_i is the angle between the unit normal \vec{N} at the point p and the vector from p to the patch A_i , θ_A is the angle between the unit normal N_A of the patch A_i and the light direction, r is the distance between the point p and the patch A_i , $H(\vec{N})$ is the hemisphere of directions around the normal \vec{N} .

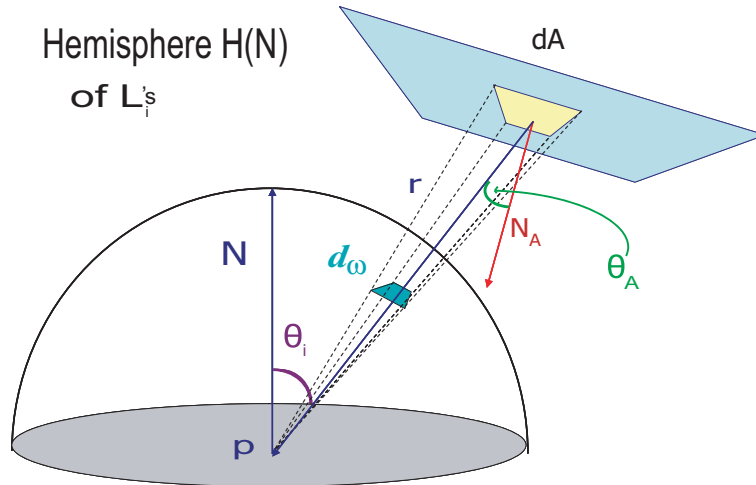


Fig. 1. Relationship between the incident light and the light leaving a point on an object surface.

In the following sections, we describe our approach to provide closed-form solutions to this integral equation. We first develop our approach for lambertian and Phong-like materials in the case of a rectangular constant area light source, which can naturally reduce to a point or a linear spot light sources. We then show that the same approach extends readily to multiple area light sources with pointwise varying color and intensity, leading thus to a unified framework that also applies to distant environment lighting using cubemaps.

A. Constant Area Light Sources

We start with this case, because its solution shows the underlying concepts in our approach, from which either specific or more general cases are derived. We derive this case for lambertian and Phong-like materials in the following sections.

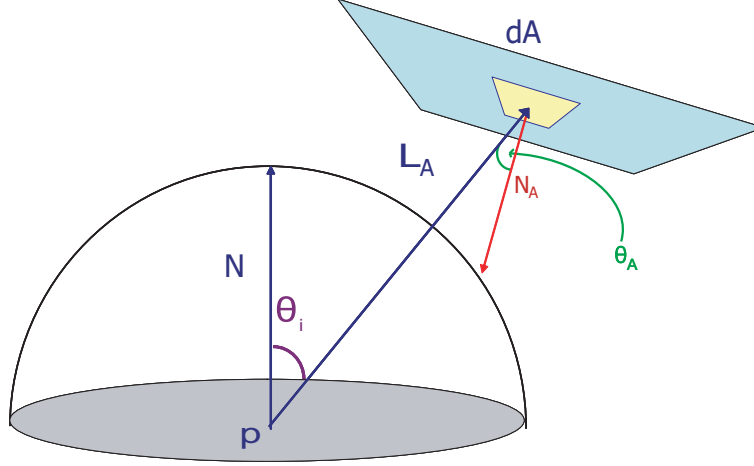


Fig. 2. Incident and irradiant light on a Lambertian surface.

1) *Lambertian Materials*: The case for perfectly diffusing Lambertian materials is shown in Figure 2. For lambertian materials, the integral assumes its simplest form:

$$L_d(p) = K_d(p) I \int_{Area} \max(0, \cos \theta_i) \frac{\cos \theta_A}{r_A^2} dA \quad (2)$$

which can also be written as

$$L_d(p) = k_d I \int_{Area} \frac{\max(0, \frac{\vec{L}_A \cdot \vec{N}}{r_A})}{r_A^2} (\frac{-\vec{L}_A}{r_A} \cdot \vec{N}_A) dA \quad (3)$$

where $k_d = K_d(p)$ is the material albedo as a function of the point p , I is the light intensity, \vec{N} is the unit normal to the surface at point p , \vec{N}_A is the unit normal to the patch dA , \vec{L}_A is the opposite direction of the light emitted by the patch dA , θ_i is the angle between \vec{N} and \vec{L}_A , θ_A is the angle between \vec{N}_A and $-\vec{L}_A$, r_A is the distance between the point p and the patch dA .

Let $d_p = r^2$ be the squared average distance between the area light source and the point p . For typical distant light sources, r_A can be replaced in practice by r with negligible error, in which case the integral reduces to

$$L_d(p) = \frac{-k_d I}{d_p^2} \int_{Area} \max(0, \vec{L}_A \cdot \vec{N}) (\vec{L}_A \cdot \vec{N}_A) dA \quad (4)$$

To simplify the above integral, we transform the endpoints a_u , b_u and c_u of the area light source and its unit normal \vec{N}_{Au} such that the surface point p is at the origin and the surface unit normal \vec{N} at the point p is along the Z-axis. We denote the transformed endpoints by a , b and c , and the transformed normal by N_A .

Let c_A be the center of the patch dA after applying the transformation, then L_A is the vector $c_A - p$. Since p is transformed to the point $(0, 0, 0)$, L_A becomes the vector $\vec{c}_A = (x_A, y_A, z_A)$, which reduces the integral to

$$L_d(p) = \frac{-k_d I}{d_p^2} \int_{Area} \max(0, \vec{c}_A \cdot \vec{N}) (\vec{c}_A \cdot \vec{N}_A) dA \quad (5)$$

Since $\vec{c}_A = (x_A, y_A, z_A)$ and $\vec{N} = (0, 0, 1)$, we have $\vec{N} \cdot \vec{c}_A = z_A$, and the integral becomes

$$L_d(p) = \frac{-k_d I}{d_p^2} \int_{Area} \max(0, z_A) (\vec{c}_A \cdot \vec{N}_A) dA \quad (6)$$

The point c_A on the rectangular area light source can be described in parametric form by $\vec{c}_A = a + u(b - a) + v(c - a)$, where $0 \leq u, v \leq 1$. The integral now becomes

$$L_d(p) = \frac{-k_d I}{d_p^2} \int_u \int_v \max(0, a_z + u(b_z - a_z) + v(c_z - a_z))$$

$$[N_{A_x} N_{A_y} N_{A_z}] \begin{bmatrix} a_x + u(b_x - a_x) + v(c_x - a_x) \\ a_y + u(b_y - a_y) + v(c_y - a_y) \\ a_z + u(b_z - a_z) + v(c_z - a_z) \end{bmatrix} dv du \quad (7)$$

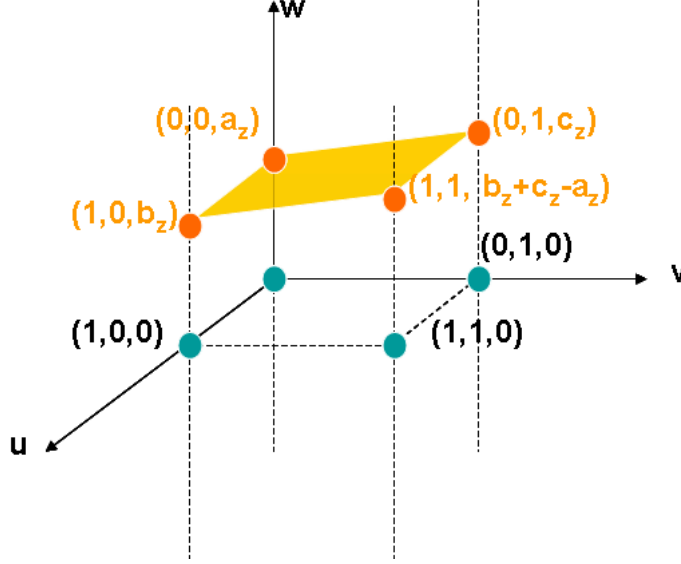


Fig. 3. The plane defining the limits of the light integral.

The above formula contains a max term that needs to be eliminated in order to be able to integrate in closed-form. The key observation that allows us to do this is the fact that $w = a + u(b - a) + v(c - a)$ is the equation of a plane as shown in Figure 3. As u and v vary in the unit interval, a plane segment is defined, whose corners are given by

u	v	w
0	0	a_z
0	1	c_z
1	0	b_z
1	1	$b_z + c_z - a_z$

The max term can be eliminated by identifying the portion of this plane segment that lies above the plane $w = 0$, i.e. by setting the bounds $u_0 \leq u \leq u_1$ and $v_0 \leq v \leq v_1$ of the integral such that only the portion above the plane $w = 0$ is taken into account. This is verified per point on the object being rendered. There are two trivial cases. The first is when all of the plane segment is above the plane $w = 0$. In this case, the bounds would be $u_0 = v_0 = 0$, and $u_1 = v_1 = 1$. The second case would be it is all under the plane $w = 0$. In this case the integral evaluates to zero.

Table I shows the bounds for each of the other cases, where $u_{line} = \frac{c_z - a_z}{a_z - b_z} v + \frac{a_z}{a_z - b_z}$, $v_{line} = \frac{b_z - a_z}{a_z - c_z} u + \frac{a_z}{a_z - c_z}$ and $d_z = b_z + c_z - a_z$. Note that the bounds of the integral are given in terms of the transformed coordinates of the end points of the area light source, which are known values. For some cases, the integral has to be divided into two subintegrals. For those cases the bounds for the first subintegral are denoted by u_0, u_1, v_0 and v_1 and the bounds for the second subintegral are denoted by u_{00}, u_{11}, v_{00} and v_{11} .

Once the bounds of the integral are determined as discussed above, the max term is simply eliminated by the fact that we would be integrating only for the cases where w is always strictly positive. Rearranging the terms in the integral then would

	u_0	u_1	v_0	v_1	u_{00}	u_{11}	v_{00}	v_{11}
$a_z \geq 0, b_z < 0,$ $c_z < 0, d_z < 0$	0	u_{line}	0	$\frac{a_z}{a_z - c_z}$				
$a_z \geq 0, b_z < 0,$ $c_z \geq 0, d_z < 0$	0	u_{line}	0	1				
$a_z \geq 0, b_z < 0,$ $c_z \geq 0, d_z \geq 0$	0	u_{line}	0	$\frac{b_z}{a_z - c_z}$	0	1	$\frac{b_z}{a_z - c_z}$	1
$a_z \geq 0, b_z \geq 0,$ $c_z < 0, d_z < 0$	0	1	0	v_{line}				
$a_z \geq 0, b_z \geq 0,$ $c_z < 0, d_z \geq 0$	0	1	0	$\frac{a_z}{a_z - c_z}$	u_{line}	1	$\frac{a_z}{a_z - c_z}$	1
$a_z \geq 0, b_z \geq 0,$ $c_z \geq 0, d_z < 0$	0	1	0	$\frac{b_z}{a_z - c_z}$	0	u_{line}	$\frac{b_z}{a_z - c_z}$	1
$a_z < 0, b_z \geq 0,$ $c_z \geq 0, d_z \geq 0$	u_{line}	1	0	$\frac{a_z}{a_z - c_z}$	0	1	$\frac{a_z}{a_z - c_z}$	1
$a_z < 0, b_z \geq 0,$ $c_z < 0, d_z \geq 0$	u_{line}	1	0	1				
$a_z < 0, b_z \geq 0,$ $c_z < 0, d_z < 0$	u_{line}	1	0	$\frac{b_z}{a_z - c_z}$				
$a_z < 0, b_z < 0,$ $c_z \geq 0, d_z \geq 0$	0	1	v_{line}	1				
$a_z < 0, b_z < 0,$ $c_z \geq 0, d_z < 0$	0	u_{line}	$\frac{a_z}{a_z - c_z}$	1				
$a_z < 0, b_z < 0,$ $c_z < 0, d_z \geq 0$	u_{line}	1	$\frac{b_z}{a_z - c_z}$	1				

TABLE I
TABLE OF INTEGRAL BOUNDS.

yield

$$L_d(p) = \frac{-k_d I}{d_p^2} \int_{u=u_0}^{u_1} \int_{v=v_0}^{v_1} (l_{00} + l_{01}v + l_{02}v^2 + l_{10}u + l_{11}uv + l_{20}u^2) dv du$$

$$\begin{aligned}
l_{00} &= a_z \times (\vec{a} \cdot \vec{N}_A) \\
l_{01} &= a_z \times ((\vec{c} - \vec{a}) \cdot \vec{N}_A) + (c_z - a_z) \times (\vec{a} \cdot \vec{N}_A) \\
l_{02} &= (c_z - a_z) \times ((\vec{c} - \vec{a}) \cdot \vec{N}_A) \\
l_{10} &= a_z \times ((\vec{b} - \vec{a}) \cdot \vec{N}_A) + (b_z - a_z) \times (\vec{a} \cdot \vec{N}_A) \\
l_{11} &= (c_z - a_z) \times ((\vec{c} - \vec{a}) \cdot \vec{N}_A) + (c_z - a_z) \times ((\vec{b} - \vec{a}) \cdot \vec{N}_A) \\
l_{20} &= (b_z - a_z) \times ((\vec{b} - \vec{a}) \cdot \vec{N}_A)
\end{aligned} \tag{8}$$

which is simply an integral of a polynomial that can be easily evaluated in closed-form. The resultant solution can then be embedded in the rendering code achieving a complexity of $O(1)$.

2) *Phong-Like Materials*: For Phong-like materials the light integral becomes as follows:

$$L_s(p) = -k_s I \int_{Area} \frac{\max(0, \frac{\vec{L}_A \cdot \vec{R}}{r_A} \cdot \vec{R})^{sh}}{r_A^2} (\frac{\vec{L}_A}{r_A} \cdot \vec{N}_A) dA \tag{9}$$

Where k_s is the albedo, sh is the shininess of the material, and \vec{R} is the reflection of the viewing vector at a point p on the surface.

Substituting r_A^2 with d_p , the integral becomes

$$L_s(p) = \frac{-k_s I}{d_p^{(sh+3)/2}} \int_{Area} \max(0, (\vec{L}_A \cdot \vec{R})^{sh}) (\vec{L}_A \cdot \vec{N}_A) dA \tag{10}$$

For Phong-like materials, we similarly transform the endpoints a_u , b_u and c_u of the area light source and its unit normal \vec{N}_{A_u} such that the surface point p is at the origin and the reflection vector \vec{R} at the point p is along the z-axis.

To simplify the integral, we proceed as we did with the Lambertian materials. The integral becomes

$$L_s(p) = \frac{-k_s I}{d_p^{(sh+3)/2}} \int_{Area} \max(0, (z_A)^{sh}) (\vec{c}_A \cdot \vec{N}_A) dA \tag{11}$$

Again, to eliminate the max term, we divide the integral into the same cases mentioned above. The integral now becomes

$$L_s(p) = \frac{-k_s I}{d_p^{(sh+3)/2}} \int_{u=u_0}^{u_1} \int_{v=v_0}^{v_1} (a_z + u(b_z - a_z) + v(c_z - a_z))^{sh} [N_{A_x} N_{A_y} N_{A_z}] \begin{bmatrix} a_x + u(b_x - a_x) + v(c_x - a_x) \\ a_y + u(b_y - a_y) + v(c_y - a_y) \\ a_z + u(b_z - a_z) + v(c_z - a_z) \end{bmatrix} dvdu \quad (12)$$

Using the trinomial expansion

$$(x + y + z)^n = \sum_{k=0}^n \sum_{l=0}^{n-k} \binom{n}{k} \binom{n-k}{l} x^{n-l-k} y^l z^k \quad (13)$$

The integral then reduces to

$$L_s(p) = \frac{-k_s I}{d_p^{(sh+3)/2}} \int_{u=u_0}^{u_1} \int_{v=v_0}^{v_1} \sum_{k=0}^{sh} \sum_{l=0}^{sh-k} \binom{sh}{k} \binom{sh-k}{l} a_z^{sh-l-k} (b_z - a_z)^l (c_z - a_z)^k u^l v^k [N_{A_x} N_{A_y} N_{A_z}] \begin{bmatrix} a_x + u(b_x - a_x) + v(c_x - a_x) \\ a_y + u(b_y - a_y) + v(c_y - a_y) \\ a_z + u(b_z - a_z) + v(c_z - a_z) \end{bmatrix} dvdu \quad (14)$$

Rearranging the terms, the integral finally becomes

$$L_s(p) = \frac{-k_s I}{d_p^{(sh+3)/2}} \sum_{k=0}^{sh} \sum_{l=0}^{sh-k} \binom{sh}{k} \binom{sh-k}{l} a_z^{sh-l-k} (b_z - a_z)^l (c_z - a_z)^k u^l v^k \int_{u=u_0}^{u_1} \int_{v=v_0}^{v_1} a_0 u^l v^k + a_1 u^{l+1} v^k + a_2 u^l v^{k+1} dvdu \quad (15)$$

$$\begin{aligned} a_0 &= \vec{N}_A \cdot \vec{a} \\ a_1 &= \vec{N}_A \cdot (\vec{b} - \vec{a}) \\ a_2 &= \vec{N}_A \cdot (\vec{c} - \vec{a}) \end{aligned}$$

which is a sum of integrals of polynomials that can be again readily evaluated in closed-form achieving a complexity of $O(sh^2)$ for Phong-like materials.

B. Non-Constant Area Light Sources

In the previous sections, we derived closed-form solutions for rendering various types of materials lit by a constant area light source of rectangular shape. These solutions reduce to a point spot light or a linear spot light source by simple dimensionality reduction. Therefore, our close-form solutions nicely include other popular light source models. To demonstrate that our approach is general, we now show that it can also be equally extended to provide a solution for direct lighting in scenes lit by environment cubemaps. Indeed, from the point of view presented in this paper, each side of a cubemap is simply an area light source with pointwise varying color and intensity. Therefore, we would simply require to extend the results in the previous sections to the case of non-constant area light sources.

We demonstrate the basic idea for Lambertian materials, which can also be extended in a similar manner as before to other types of material. For Lambertian materials the light integral becomes

$$L_d(p) = k_d \int_{Area} I_A \max(0, \cos \theta_i) \frac{\cos \theta_A}{r_A^2} dA \quad (16)$$

Following the same steps as before the integral can be simplified to

$$L_d(p) = \frac{-k_d}{d^2} \int_{u=u_0}^{u_1} \int_{v=v_0}^{v_1} I(u, v) (l_{00} + l_{01}v + l_{02}v^2 + l_{10}u + l_{11}uv + l_{20}u^2) dvdu$$

$$\begin{aligned}
l_{00} &= a_z \times (\vec{a} \cdot \vec{N}_A) \\
l_{01} &= a_z \times ((\vec{c} - \vec{a}) \cdot \vec{N}_A) + (c_z - a_z) \times (\vec{a} \cdot \vec{N}_A) \\
l_{02} &= (c_z - a_z) \times ((\vec{c} - \vec{a}) \cdot \vec{N}_A) \\
l_{10} &= a_z \times ((\vec{b} - \vec{a}) \cdot \vec{N}_A) + (b_z - a_z) \times (\vec{a} \cdot \vec{N}_A) \\
l_{11} &= (c_z - a_z) \times ((\vec{c} - \vec{a}) \cdot \vec{N}_A) + (c_z - a_z) \times ((\vec{b} - \vec{a}) \cdot \vec{N}_A) \\
l_{20} &= (b_z - a_z) \times ((\vec{b} - \vec{a}) \cdot \vec{N}_A)
\end{aligned} \tag{17}$$

where $I(u, v)$ is the varying light color and intensity, which is essentially a pixel in an image of a cubemap.

This integral can be solved in closed-form only if we can provide a closed-form expression for the pixel value $I(u, v)$. A natural way to do this would be to use some basis function. In principle, any basis may be used to compute $I(u, v)$. However, we used the Discrete Cosine Transform (DCT), since it provides two advantages. First, combined with the light integral equation, it lends itself to a closed-form solution, second DCT is a well established and widely used compression tool. Therefore $I(u, v)$ is given by an inverse cosine transform of a set of coefficients precomputed by preprocessing the image in the cubemap, as follows:

$$\begin{aligned}
I(u, v) &= \sum_{i=0}^{N-1} \sum_{j=0}^{M-1} \alpha_i \alpha_j C_{ij} \cos(k_{i0}u + k_{i1}) \cos(k_{j0}v + k_{j1}) \\
\text{where } \alpha_i &= \begin{cases} 1/\sqrt{N}, i = 0 \\ \sqrt{2/N}, 1 \leq i \leq N-1 \end{cases} \\
\alpha_j &= \begin{cases} 1/\sqrt{M}, j = 0 \\ \sqrt{2/M}, 1 \leq j \leq M-1 \end{cases} \\
k_{i0} &= \pi i(N-1)/N, \quad k_{j0} = \pi j(M-1)/M \\
k_{i1} &= \pi i/2N, \quad k_{j1} = \pi j/2M
\end{aligned} \tag{18}$$

The C_{ij} 's are the DCT coefficients. The coefficients are precomputed for each color channel and are stored as a cubemap that is used as an input to our rendering equation in (17). The preprocessing step requires $N_c \log(N_c)$ time, if we use N_c coefficients.

Upon substituting from (18) into (17), our integral becomes

$$\begin{aligned}
L_d(p) &= \frac{-k_d}{d^2} \int_{u=u_0}^{u_1} \int_{v=v_0}^{v_1} \sum_{i=0}^{N-1} \sum_{j=0}^{M-1} \alpha_i \alpha_j C_{ij} \\
&\quad \cos(k_{i0}u + k_{i1}) \cos(k_{j0}v + k_{j1}) \\
&\quad (l_{00} + l_{01}v + l_{02}v^2 + l_{10}u + l_{11}uv + l_{20}u^2) dvdu
\end{aligned} \tag{19}$$

We then rearrange the integral to get the following

$$\begin{aligned}
L_d(p) &= \frac{-k_d}{d^2} \sum_{i=0}^{N-1} \sum_{j=0}^{M-1} \alpha_i \alpha_j C_{ij} \int_{u=u_0}^{u_1} \int_{v=v_0}^{v_1} \\
&\quad \cos(k_{i0}u + k_{i1}) \cos(k_{j0}v + k_{j1}) \\
&\quad (l_{00} + l_{01}v + l_{02}v^2 + l_{10}u + l_{11}uv + l_{20}u^2) dvdu
\end{aligned} \tag{20}$$

A closed-form solution can now be found for the integral part of the above equation, which we denote by \mathfrak{S}_{ij} . The closed form generated will have divisions by the constants k_{i0} , k_{i1} , k_{j0} and k_{j1} . However, at $i=0$ and $j=0$ these constants evaluate to zero, leading to divisions by zero. To solve this problem, the integral is divided into four cases:

1) Case 1: $i \neq 0$ and $j \neq 0$

$$\begin{aligned}
I_{ij} &= \int_{u=u_0}^{u_1} \int_{v=v_0}^{v_1} \cos(k_{i0}u + k_{i1}) \cos(k_{j0}v + k_{j1}) \\
&\quad (l_{00} + l_{01}v + l_{02}v^2 + l_{10}u + l_{11}uv + l_{20}u^2) dvdu
\end{aligned} \tag{21}$$

2) Case 2: $i = 0$ and $j \neq 0$

$$\begin{aligned}
I_{0j} &= \int_{u=u_0}^{u_1} \int_{v=v_0}^{v_1} \cos(k_{j0}v + k_{j1}) \\
&\quad (l_{00} + l_{01}v + l_{02}v^2 + l_{10}u + l_{11}uv + l_{20}u^2) dvdu
\end{aligned} \tag{22}$$

3) Case 3: $i \neq 0$ and $j = 0$

$$I_{i0} = \int_{u=u_0}^{u_1} \int_{v=v_0}^{v_1} \cos(k_{i0}u + k_{i1}) (l_{00} + l_{01}v + l_{02}v^2 + l_{10}u + l_{11}uv + l_{20}u^2) dvdu \quad (23)$$

4) Case 4: $i = 0$ and $j = 0$

$$I_{00} = \int_{u=u_0}^{u_1} \int_{v=v_0}^{v_1} (l_{00} + l_{01}v + l_{02}v^2 + l_{10}u + l_{11}uv + l_{20}u^2) dvdu \quad (24)$$

which is the same as the constant area light source for lambertian materials case.

The above integrals can now be evaluated using the bounds in table-2 and the color value at a point p on a Lambertian surface will be

$$L_d(p) = \frac{-k_d}{d^2} \sum_{i=0}^{N-1} \sum_{j=0}^{M-1} \alpha_i \alpha_j C_{ij} \mathfrak{S}_{ij} \quad (25)$$

where,

$$\mathfrak{S}_{ij} = \begin{cases} I_{ij}, & i \neq 0 \ \& \ j \neq 0 \\ I_{0j}, & i = 0 \ \& \ j \neq 0 \\ I_{i0}, & i \neq 0 \ \& \ j = 0 \\ I_{00}, & i = 0 \ \& \ j = 0 \end{cases}$$

The number of coefficients generated by the discrete cosine transform of the image is equal to the image resolution $M \times N$. If desired, all $M \times N$ coefficients can be used to compute $L_o(p)$ in $O(MN)$ time, or alternatively we can truncate the coefficients to some desired cut-off low frequency values trading between accuracy and speed.

The nature of our closed-form solution allows our algorithm to work for high frequency as well as low frequency. Another significant advantage is that we are able to achieve realistic shading using only *one* coefficient per face, reducing the number of coefficients needed to achieve realistic shading as compared to spherical harmonics.

If $O(1)$ complexity is desired, the analytic solution for the lambertian surfaces under constant lighting can be used, such that $I = C_{00}/\sqrt{MN}$.

IV. RESULTS AND DISCUSSION

We have applied and verified our method under various lighting scenarios for lambertian and Phong-like materials. For constant lighting Figure 6 displays Lambertian and Phong-like materials under such lighting. Figure 7 demonstrates the variations in the shininess of the material lit by an area light source. Figures 8, 9 and 10 show examples of rendering lambertian objects in different environments. As mentioned earlier, all lambertian objects are rendered at $O(1)$ time complexity. For environment lighting, one can readily see in Figures 8, 9 and 10 that our method realistically captures the effect of colors in the environment on the rendered objects.

To evaluate the quality of our results, we performed three sets of experiments. The first set establishes the error associated with the approximation that led to our closed-form solution, i.e. the assumption that the distance between the point being shaded and the light patch dA is constant and equal to the average distance. We varied the ratio of the squared distance over the area of the light source, $d^2/Area$, and generated ground truth images under illumination with area light sources at finite distances, using the Monte Carlo technique with more than 1000 samples. Then, images under the exact same lighting conditions were generated using our method. The images were compared with the ground truth in the HSI domain to avoid the color channel correlations of the RGB model. Figures 4 - (a) and (b) show the results for the Saturation channel. As for the Hue and Intensity channels, we found 0% error indicating that for our method they are independent of the ratio $d^2/Area$. As shown in these figures, the peak-signal-to-noise ratio (PSNR) increases as a function of $d^2/Area$, or equivalently the relative error reduces as this ratio increases. Note that the PSNR increases sharply to about 40dB for $d^2/Area < 1$, and remains approximately stable thereafter. Note also that even for small values of $d^2/Area = 0.4$, the PSNR for our method has a remarkably high value of over 33dB.

In the second set of experiments, we generated ground truth images by rendering a lambertian sphere in several cubemaps, i.e. under distant environment lighting. We then rendered images of the sphere under the same lighting using our method. We tested for both SNR and relative error against the ground-truth generated by Monte Carlo, and averaged over a large number of environments. Results are summarized in Table II. We observed that for lambertian materials the lower-bound in the relative error (or the upper-bound for SNR) is achieved with one coefficient per face in our method. In other words, we achieve our best result with the DC value of the cosine transform, and our method is almost invariant to the frequency of light in the case of lambertian material.

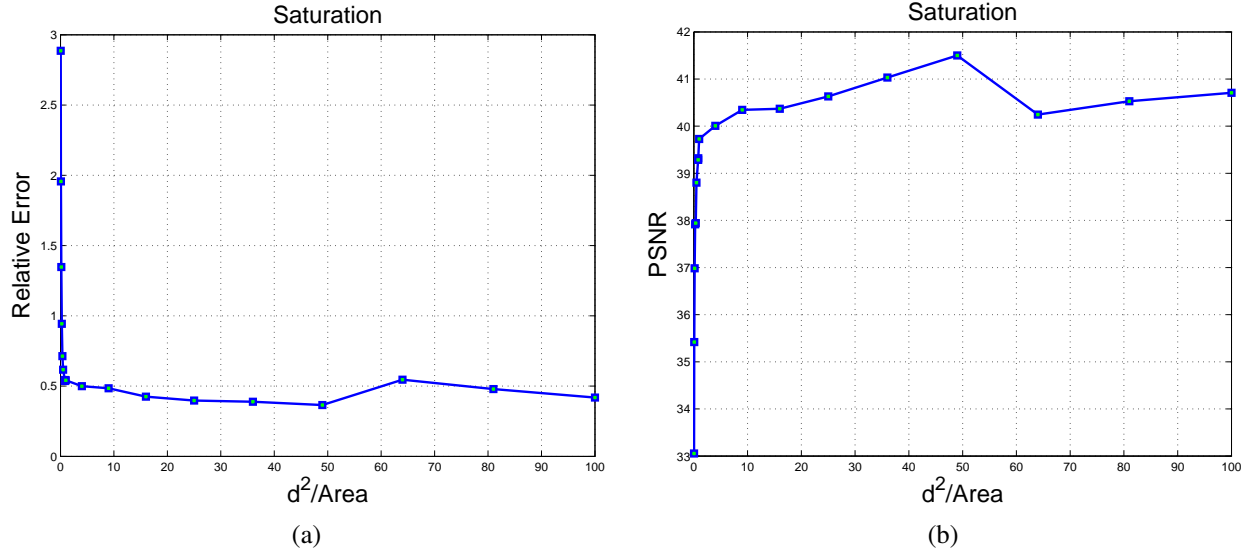


Fig. 4. (a) Percentage relative error of our method against Monte Carlo, (b) Peak-Signal-to-noise error of our method against Monte Carlo

RGB: Relative Error	HSI: Relative Error	HSI: SNR (dB)
R=0.0075%	H=0.0161%	H=42.5401
G=0.0075%	S=0.3614%	S=54.9891
B=0.0049%	I=0%	I= ∞

TABLE II
ERRORS AND SNR FOR DIFFERENT COLOR CHANNELS AVERAGED OVER SEVERAL OBJECTS IN DIFFERENT ENVIRONMENTS.

In the third set of experiments, we generated ground truth images for multiple environments using Monte Carlo, with more than 1000 samples. We generated images under the same environments using Spherical Harmonics and our method. The error was computed against the ground truth provided by Monte Carlo. Figures 5- (a) and (b) show the results for one of the environments used in the experiment. By examining the figures one can tell that our method provides more accurate results than Spherical Harmonics.

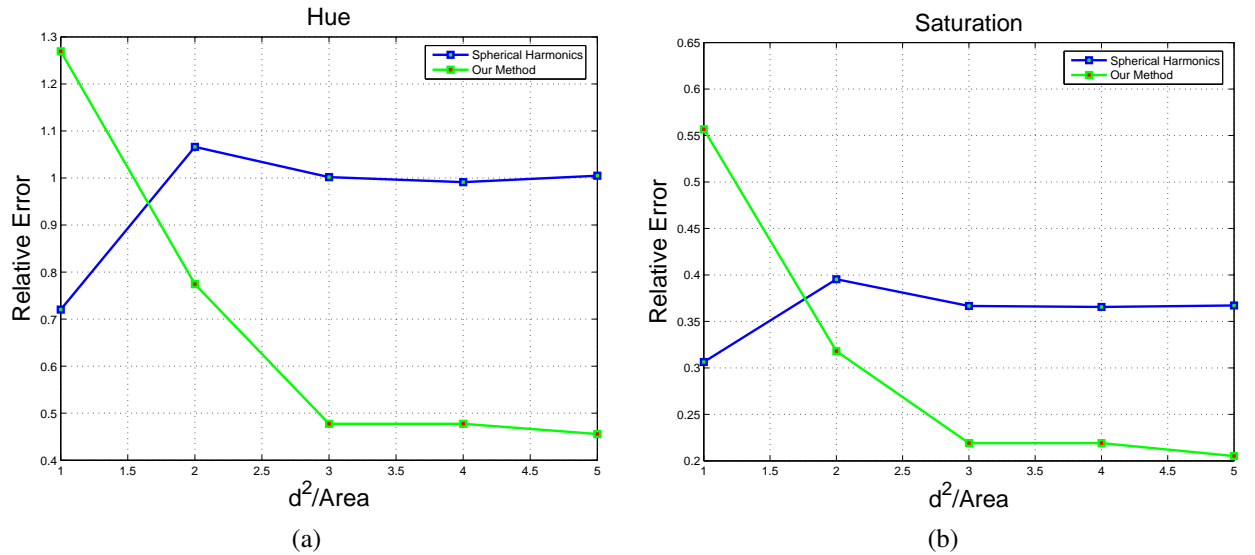


Fig. 5. (a) Hue Percentage relative error of Spherical Harmonics and our method against Monte Carlo, (b) Saturation Percentage relative error of Spherical Harmonics and our method against Monte Carlo

In summary, we first formulated a novel approach to provide closed-form solutions to the light integral for lambertian and Phong-like materials, which are lit by constant area light sources. Spot light and directional linear light sources are then special cases of our formulation. Using the key observation that a cubemap can be represented as six non-constant area light sources,

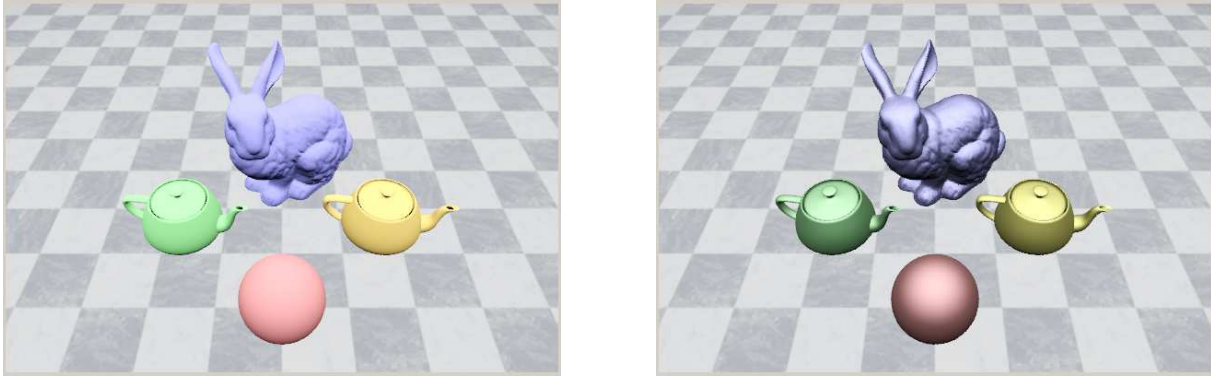


Fig. 6. Lambertian and Phong-like materials lit by a constant area light source

we have also shown that the same framework can be extended to provide a closed-form solution to environment lighting. In our formulation, the cut-off frequency of the light can be chosen arbitrarily at any desired value in the cosine transform domain. In particular, for lambertian material, we only require one DCT coefficient per face to render realistic images, achieving a complexity of $O(1)$. Also, we gain an order of magnitude or higher in rendering time compared to classical environment sampling techniques such as Monte Carlo.

In principle, models of other material types can be formulated within our framework and solved in similar fashions. Another direction of research could be the incorporation of general BRDFs. One issue that needs to be considered is the rendering of shadows. In classical estimation techniques based on sampling, shadowing is implicitly incorporated. In our framework, due to the closed-form nature of our solution, shadows need to be computed explicitly. However, several methods have already been proposed in the existing literature [53], [55], [138] for efficient and realistic computation of shadows that would nicely fit in our framework.

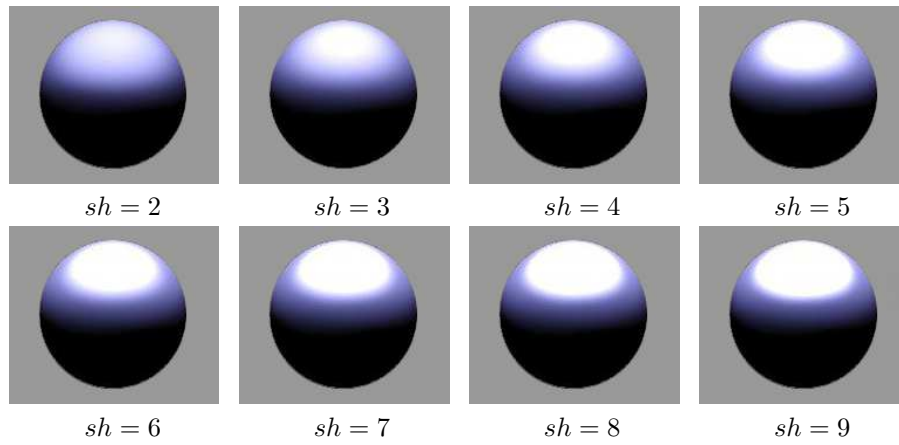


Fig. 7. Examples of rendering Phong-like material with different shininess parameters under an area light source.



Fig. 8. Lambertian buddha lit by different environments



Fig. 9. Lambertian dragon lit by different environments



Fig. 10. Lambertian kangaroo lit by different environments

APPENDIX

The following is *pseudo code* for implementing the algorithm. It is intended to provide a global understanding of our algorithm.

For each point p to be rendered

if (lambertian){

Transform the end points of the light source a_u , b_u and c_u and its normal N_{A_u} such that the point p is at the origin and the unit normal \vec{N} at the point p is along the z -axis.

Compute l_{00} , l_{01} , l_{02} , l_{10} , l_{11} , l_{20}

if($a_z \geq 0$ and $b_z < 0$ and $c_z < 0$ and $d_z < 0$)

if(Constant)

call formula for constant_diff_case1.

else

for each of the six faces of the cube map call formula for nonconstant_diff_case1.

else if($a_z \geq 0$ and $b_z < 0$ and $c_z \geq 0$ and $d_z < 0$)

if(Constant)

call formula for constant_diff_case2.

else

for each of the six faces of the cube map call formula for nonconstant_diff_case2.

else if(...)

:

else if($a_z < 0$ and $b_z < 0$ and $c_z < 0$ and $d_z < 0$)

return 0

}

else if(specular){

Transform the end points of the light source a_u , b_u and c_u and its normal N_{A_u} such that the point p is at the origin and the reflection vector \vec{R} at the point p is along the z -axis.

Compute l_{00} , l_{01} , l_{02} , l_{10} , l_{11} , l_{20}

if($a_z \geq 0$ and $b_z < 0$ and $c_z < 0$ and $d_z < 0$)

call formula for constant_spec_case1.

if($a_z \geq 0$ and $b_z < 0$ and $c_z \geq 0$ and $d_z < 0$)

call formula for constant_spec_case2.

else if(...)

:

else if($a_z < 0$ and $b_z < 0$ and $c_z < 0$ and $d_z < 0$)

return 0

}

REFERENCES

- [1] Muhamad Ali and Hassan Foroosh. Natural scene character recognition without dependency on specific features. In *Proc. International Conference on Computer Vision Theory and Applications*, 2015.
- [2] Muhamad Ali and Hassan Foroosh. A holistic method to recognize characters in natural scenes. In *Proc. International Conference on Computer Vision Theory and Applications*, 2016.
- [3] Muhammad Ali and Hassan Foroosh. Character recognition in natural scene images using rank-1 tensor decomposition. In *Proc. of International Conference on Image Processing (ICIP)*, pages 2891–2895, 2016.
- [4] Mais Alnasser and Hassan Foroosh. Image-based rendering of synthetic diffuse objects in natural scenes. In *Proc. IAPR Int. Conference on Pattern Recognition*, volume 4, pages 787–790, 2006.
- [5] Mais Alnasser and Hassan Foroosh. Rendering synthetic objects in natural scenes. In *Proc. of IEEE International Conference on Image Processing (ICIP)*, pages 493–496, 2006.
- [6] Mais Alnasser and Hassan Foroosh. Phase shifting for non-separable 2d haar wavelets. *IEEE Transactions on Image Processing*, 16:1061–1068, 2008.
- [7] James Arvo. The irradiance Jacobian for partially occluded polyhedral sources. In *Computer Graphics Proceedings, Annual Conference Series, ACM SIGGRAPH*, pages 343–350, July 1994.
- [8] Nazim Ashraf and Hassan Foroosh. Robust auto-calibration of a ptz camera with non-overlapping fov. In *Proc. International Conference on Pattern Recognition (ICPR)*, 2008.
- [9] Nazim Ashraf and Hassan Foroosh. Human action recognition in video data using invariant characteristic vectors. In *Proc. of IEEE Int. Conf. on Image Processing (ICIP)*, pages 1385–1388, 2012.
- [10] Nazim Ashraf and Hassan Foroosh. Motion retrieval using consistency of epipolar geometry. In *Proceedings of IEEE International Conference on Image Processing (ICIP)*, pages 4219–4223, 2015.
- [11] Nazim Ashraf, Imran Junejo, and Hassan Foroosh. Near-optimal mosaic selection for rotating and zooming video cameras. *Proc. of Asian Conf. on Computer Vision*, pages 63–72, 2007.
- [12] Nazim Ashraf, Yuping Shen, Xiaochun Cao, and Hassan Foroosh. View-invariant action recognition using weighted fundamental ratios. *Journal of Computer Vision and Image Understanding (CVIU)*, 117:587–602, 2013.
- [13] Nazim Ashraf, Yuping Shen, Xiaochun Cao, and Hassan Foroosh. View invariant action recognition using weighted fundamental ratios. *Computer Vision and Image Understanding*, 117(6):587–602, 2013.
- [14] Nazim Ashraf, Yuping Shen, and Hassan Foroosh. View-invariant action recognition using rank constraint. In *Proc. of IAPR Int. Conf. Pattern Recognition (ICPR)*, pages 3611–3614, 2010.
- [15] Nazim Ashraf, Chuan Sun, and Hassan Foroosh. Motion retrieval using low-rank decomposition of fundamental ratios. In *Proc. IEEE International Conference on Image Processing (ICIP)*, pages 1905–1908, 2012.
- [16] Nazim Ashraf, Chuan Sun, and Hassan Foroosh. Motion retrieval using low-rank decomposition of fundamental ratios. In *Image Processing (ICIP), 2012 19th IEEE International Conference on*, pages 1905–1908, 2012.
- [17] Nazim Ashraf, Chuan Sun, and Hassan Foroosh. View-invariant action recognition using projective depth. *Journal of Computer Vision and Image Understanding (CVIU)*, 123:41–52, 2014.
- [18] Nazim Ashraf, Chuan Sun, and Hassan Foroosh. View invariant action recognition using projective depth. *Computer Vision and Image Understanding*, 123:41–52, 2014.
- [19] Vildan Atalay and Hassan Foroosh. In-band sub-pixel registration of wavelet-encoded images from sparse coefficients. *Signal, Image and Video Processing*, 2017.
- [20] Vildan A. Aydin and Hassan Foroosh. Motion compensation using critically sampled dwt subbands for low-bitrate video coding. In *Proc. IEEE International Conference on Image Processing (ICIP)*, 2017.
- [21] Murat Balci, Mais Alnasser, and Hassan Foroosh. Alignment of maxillofacial ct scans to stone-cast models using 3d symmetry for backscattering artifact reduction. In *Proceedings of Medical Image Understanding and Analysis Conference*, 2006.
- [22] Murat Balci, Mais Alnasser, and Hassan Foroosh. Image-based simulation of gaseous material. In *Proc. of IEEE International Conference on Image Processing (ICIP)*, pages 489–492, 2006.
- [23] Murat Balci, Mais Alnasser, and Hassan Foroosh. Subpixel alignment of mri data under cartesian and log-polar sampling. In *Proc. of IAPR Int. Conf. Pattern Recognition*, volume 3, pages 607–610, 2006.
- [24] Murat Balci and Hassan Foroosh. Estimating sub-pixel shifts directly from phase difference. In *Proc. of IEEE International Conference on Image Processing (ICIP)*, pages 1057–1060, 2005.
- [25] Murat Balci and Hassan Foroosh. Estimating sub-pixel shifts directly from the phase difference. In *Proc. of IEEE Int. Conf. Image Processing (ICIP)*, volume 1, pages 1–1057, 2005.
- [26] Murat Balci and Hassan Foroosh. Inferring motion from the rank constraint of the phase matrix. In *Proc. IEEE Conf. on Acoustics, Speech, and Signal Processing*, volume 2, pages ii–925, 2005.
- [27] Murat Balci and Hassan Foroosh. Metrology in uncalibrated images given one vanishing point. In *Proc. of IEEE International Conference on Image Processing (ICIP)*, pages 361–364, 2005.
- [28] Murat Balci and Hassan Foroosh. Real-time 3d fire simulation using a spring-mass model. In *Proc. of Int. Multi-Media Modelling Conference*, pages 8–pp, 2006.
- [29] Murat Balci and Hassan Foroosh. Sub-pixel estimation of shifts directly in the fourier domain. *IEEE Trans. on Image Processing*, 15(7):1965–1972, 2006.
- [30] Murat Balci and Hassan Foroosh. Sub-pixel registration directly from phase difference. *Journal of Applied Signal Processing-special issue on Super-resolution Imaging*, 2006:1–11, 2006.
- [31] M Berthod, M Werman, H Shekarforoush, and J Zerubia. Refining depth and luminance information using super-resolution. In *Proc. of IEEE Conf. Computer Vision and Pattern Recognition (CVPR)*, pages 654–657, 1994.
- [32] Marc Berthod, Hassan Shekarforoush, Michael Werman, and Josiane Zerubia. Reconstruction of high resolution 3d visual information. In *IEEE Conf. Computer Vision and Pattern Recognition (CVPR)*, pages 654–657, 1994.
- [33] Adeel Bhutta and Hassan Foroosh. Blind blur estimation using low rank approximation of cepstrum. *Image Analysis and Recognition*, pages 94–103, 2006.
- [34] Adeel A Bhutta, Imran N Junejo, and Hassan Foroosh. Selective subtraction when the scene cannot be learned. In *Proc. of IEEE International Conference on Image Processing (ICIP)*, pages 3273–3276, 2011.
- [35] Hakan Boyraz, Syed Zain Masood, Baoyuan Liu, Marshall Tappen, and Hassan Foroosh. Action recognition by weakly-supervised discriminative region localization.
- [36] Ozan Cakmakci, Gregory E. Fasshauer, Hassan Foroosh, Kevin P. Thompson, and Jannick P. Rolland. Meshfree approximation methods for free-form surface representation in optical design with applications to head-worn displays. In *Proc. SPIE Conf. on Novel Optical Systems Design and Optimization XI*, volume 7061, 2008.
- [37] Ozan Cakmakci, Brendan Moore, Hassan Foroosh, and Jannick Rolland. Optimal local shape description for rotationally non-symmetric optical surface design and analysis. *Optics Express*, 16(3):1583–1589, 2008.

- [38] Ozan Cakmakci, Sophie Vo, Hassan Foroosh, and Jannick Rolland. Application of radial basis functions to shape description in a dual-element off-axis magnifier. *Optics Letters*, 33(11):1237–1239, 2008.
- [39] X Cao and H Foroosh. Metrology from vertical objects. In *Proceedings of the British Machine Conference (BMVC)*, pages 74–1.
- [40] Xiaochun Cao and Hassan Foroosh. Camera calibration without metric information using 1d objects. In *Proc. International Conf. on Image Processing (ICIP)*, volume 2, pages 1349–1352, 2004.
- [41] Xiaochun Cao and Hassan Foroosh. Camera calibration without metric information using an isosceles trapezoid. In *Proc. International Conference on Pattern Recognition (ICPR)*, volume 1, pages 104–107, 2004.
- [42] Xiaochun Cao and Hassan Foroosh. Simple calibration without metric information using an isosceles trapezoid. In *Proc. of IAPR Int. Conf. Pattern Recognition (ICPR)*, volume 1, pages 104–107, 2004.
- [43] Xiaochun Cao and Hassan Foroosh. Camera calibration using symmetric objects. *IEEE Transactions on Image Processing*, 15(11):3614–3619, 2006.
- [44] Xiaochun Cao and Hassan Foroosh. Synthesizing reflections of inserted objects. In *Proc. IAPR Int. Conference on Pattern Recognition*, volume 2, pages 1225–1228, 2006.
- [45] Xiaochun Cao and Hassan Foroosh. Camera calibration and light source orientation from solar shadows. *Journal of Computer Vision & Image Understanding (CVIU)*, 105:60–72, 2007.
- [46] Xiaochun Cao, Wenqi Ren, Wangmeng Zuo, Xiaojie Guo, and Hassan Foroosh. Scene text deblurring using text-specific multi-scale dictionaries. *IEEE Transactions on Image Processing*, 24(4):1302–1314, 2015.
- [47] Xiaochun Cao, Yuping Shen, Mubarak Shah, and Hassan Foroosh. Single view compositing with shadows. *The Visual Computer*, 21(8-10):639–648, 2005.
- [48] Xiaochun Cao, Lin Wu, Jiangjian Xiao, Hassan Foroosh, Jigui Zhu, and Xiaohong Li. Video synchronization and its application on object transfer. *Image and Vision Computing (IVC)*, 28(1):92–100, 2009.
- [49] Xiaochun Cao, Jiangjian Xiao, and Hassan Foroosh. Camera motion quantification and alignment. In *Proc. International Conference on Pattern Recognition (ICPR)*, volume 2, pages 13–16, 2006.
- [50] Xiaochun Cao, Jiangjian Xiao, and Hassan Foroosh. Self-calibration using constant camera motion. In *Proc. of IAPR Int. Conf. Pattern Recognition (ICPR)*, volume 1, pages 595–598, 2006.
- [51] Xiaochun Cao, Jiangjian Xiao, Hassan Foroosh, and Mubarak Shah. Self-calibration from turn table sequence in presence of zoom and focus. *Computer Vision and Image Understanding (CVIU)*, 102(3):227–237, 2006.
- [52] Min Chen and James Arvo. A closed-form solution for the irradiance due to linearly-varying luminaires. In *Proceedings of the Eurographics Workshop on Rendering Techniques 2000*, pages 137–148, London, UK, 2000. Springer-Verlag.
- [53] N. Chin and S. Feiner. Fast object-precision shadow generation for area light sources using bsp trees. In *Proc. Symposium on Interactive 3D Graphics*, pages 21–30, 1992.
- [54] Kristian L Damkjær and Hassan Foroosh. Mesh-free sparse representation of multidimensional LIDAR data. In *Proc. of International Conference on Image Processing (ICIP)*, pages 4682–4686, 2014.
- [55] George Drettakis and Eugene Fiume. A fast shadow algorithm for area light sources using backprojection. In *SIGGRAPH '94: Proceedings of the 21st annual conference on Computer graphics and interactive techniques*, pages 223–230, New York, NY, USA, 1994. ACM Press.
- [56] Farshideh Einsele and Hassan Foroosh. Recognition of grocery products in images captured by cellular phones. In *Proc. International Conference on Computer Vision and Image Processing (ICCVIP)*, 2015.
- [57] H Foroosh. Adaptive estimation of motion using generalized cross validation. In *3rd International (IEEE) Workshop on Statistical and Computational Theories of Vision*, 2003.
- [58] Hassan Foroosh. A closed-form solution for optical flow by imposing temporal constraints. In *Proc. of IEEE International Conf. on Image Processing (ICIP)*, volume 3, pages 656–659, 2001.
- [59] Hassan Foroosh. An adaptive scheme for estimating motion. In *Proc. of IEEE International Conf. on Image Processing (ICIP)*, volume 3, pages 1831–1834, 2004.
- [60] Hassan Foroosh. Pixelwise adaptive dense optical flow assuming non-stationary statistics. *IEEE Trans. on Image Processing*, 14(2):222–230, 2005.
- [61] Hassan Foroosh and Murat Balci. Sub-pixel registration and estimation of local shifts directly in the fourier domain. In *Proc. International Conference on Image Processing (ICIP)*, volume 3, pages 1915–1918, 2004.
- [62] Hassan Foroosh and Murat Balci. Subpixel registration and estimation of local shifts directly in the fourier domain. In *Proc. of IEEE International Conference on Image Processing (ICIP)*, volume 3, pages 1915–1918, 2004.
- [63] Hassan Foroosh, Murat Balci, and Xiaochun Cao. Self-calibrated reconstruction of partially viewed symmetric objects. In *Proc. IEEE Int. Conf. on Acoustics, Speech, and Signal Processing (ICASSP)*, volume 2, pages ii–869, 2005.
- [64] Hassan Foroosh and W Scott Hoge. Motion information in the phase domain. In *Video registration*, pages 36–71. Springer, 2003.
- [65] Hassan Foroosh, Josiane Zerubia, and Marc Berthod. Extension of phase correlation to subpixel registration. *IEEE Trans. on Image Processing*, 11(3):188–200, 2002.
- [66] Tao Fu and Hassan Foroosh. Expression morphing from distant viewpoints. In *Proc. of IEEE International Conference on Image Processing (ICIP)*, volume 5, pages 3519–3522, 2004.
- [67] Wei Hu, Gene Cheung, Xin Li, and Oscar C. Au. Depth map super-resolution using synthesized view matching for depth-image-based rendering. In *IEEE International Conference on Multimedia and Expo Workshops*, pages 605–610, 2012.
- [68] Apurva Jain, Supraja Murali, Nicolene Papp, Kevin Thompson, Kye-sung Lee, Panomsak Meemon, Hassan Foroosh, and Jannick P Rolland. Super-resolution imaging combining the design of an optical coherence microscope objective with liquid-lens based dynamic focusing capability and computational methods. In *Optical Engineering & Applications*, pages 70610C–70610C. International Society for Optics and Photonics, 2008.
- [69] I Junejo, A Bhutta, and Hassan Foroosh. Dynamic scene modeling for object detection using single-class svm. In *Proc. of IEEE International Conference on Image Processing (ICIP)*, volume 1, pages 1541–1544, 2010.
- [70] Imran Junejo, Xiaochun Cao, and Hassan Foroosh. Configuring mixed reality environment. In *Proc. of IEEE International Conference on Advanced Video and Signal-based Surveillance*, pages 884–887, 2006.
- [71] Imran Junejo, Xiaochun Cao, and Hassan Foroosh. Geometry of a non-overlapping multi-camera network. In *Proc. of IEEE International Conference on Advanced Video and Signal-based Surveillance*, pages 43–48, 2006.
- [72] Imran Junejo, Xiaochun Cao, and Hassan Foroosh. Autoconfiguration of a dynamic non-overlapping camera network. *IEEE Trans. Systems, Man, and Cybernetics*, 37(4):803–816, 2007.
- [73] Imran Junejo and Hassan Foroosh. Dissecting the image of the absolute conic. In *Proc. of IEEE Int. Conf. on Video and Signal Based Surveillance*, pages 77–77, 2006.
- [74] Imran Junejo and Hassan Foroosh. Robust auto-calibration from pedestrians. In *Proc. IEEE International Conference on Video and Signal Based Surveillance*, pages 92–92, 2006.
- [75] Imran Junejo and Hassan Foroosh. Euclidean path modeling from ground and aerial views. In *Proc. International Conference on Computer Vision (ICCV)*, pages 1–7, 2007.
- [76] Imran Junejo and Hassan Foroosh. Trajectory rectification and path modeling for surveillance. In *Proc. International Conference on Computer Vision (ICCV)*, pages 1–7, 2007.
- [77] Imran Junejo and Hassan Foroosh. Using calibrated camera for euclidean path modeling. In *Proceedings of IEEE International Conference on Image Processing (ICIP)*, pages 205–208, 2007.

- [78] Imran Junejo and Hassan Foroosh. Euclidean path modeling for video surveillance. *Image and Vision Computing (IVC)*, 26(4):512–528, 2008.
- [79] Imran Junejo and Hassan Foroosh. Camera calibration and geo-location estimation from two shadow trajectories. *Computer Vision and Image Understanding (CVIU)*, 114:915–927, 2010.
- [80] Imran Junejo and Hassan Foroosh. Gps coordinates estimation and camera calibration from solar shadows. *Computer Vision and Image Understanding (CVIU)*, 114(9):991–1003, 2010.
- [81] Imran Junejo and Hassan Foroosh. Optimizing ptz camera calibration from two images. *Machine Vision and Applications (MVA)*, pages 1–15, 2011.
- [82] Imran N Junejo, Nazim Ashraf, Yuping Shen, and Hassan Foroosh. Robust auto-calibration using fundamental matrices induced by pedestrians. In *Proc. International Conf. on Image Processing (ICIP)*, volume 3, pages III–201, 2007.
- [83] Imran N. Junejo, Adeel Bhutta, and Hassan Foroosh. Single-class svm for dynamic scene modeling. *Signal Image and Video Processing*, 7(1):45–52, 2013.
- [84] Imran N Junejo, Xiaochun Cao, and Hassan Foroosh. Calibrating freely moving cameras. In *Proc. International Conference on Pattern Recognition (ICPR)*, volume 4, pages 880–883, 2006.
- [85] Imran N. Junejo and Hassan Foroosh. Trajectory rectification and path modeling for video surveillance. In *Proc. International Conference on Computer Vision (ICCV)*, pages 1–7, 2007.
- [86] Imran N. Junejo and Hassan Foroosh. Estimating geo-temporal location of stationary cameras using shadow trajectories. In *Proc. European Conference on Computer Vision (ECCV)*, 2008.
- [87] Imran N. Junejo and Hassan Foroosh. Gps coordinate estimation from calibrated cameras. In *Proc. International Conference on Pattern Recognition (ICPR)*, 2008.
- [88] Imran N Junejo and Hassan Foroosh. Gps coordinate estimation from calibrated cameras. In *Proc. International Conference on Pattern Recognition (ICPR)*, pages 1–4, 2008.
- [89] Imran N. Junejo and Hassan Foroosh. Practical ptz camera calibration using givens rotations. In *Proc. IEEE International Conference on Image Processing (ICIP)*, 2008.
- [90] Imran N. Junejo and Hassan Foroosh. Practical pure pan and pure tilt camera calibration. In *Proc. International Conference on Pattern Recognition (ICPR)*, 2008.
- [91] Imran N. Junejo and Hassan Foroosh. Refining ptz camera calibration. In *Proc. International Conference on Pattern Recognition (ICPR)*, 2008.
- [92] Imran N. Junejo and Hassan Foroosh. Using solar shadow trajectories for camera calibration. In *Proc. IEEE International Conference on Image Processing (ICIP)*, 2008.
- [93] Malvin H. Kalos and Paula A. Whitlock. *Monte Carlo methods. Vol. 1: basics*. Wiley-Interscience, New York, NY, USA, 1986.
- [94] Anne Lorette, Hassan Shekarforoush, and Josiane Zerubia. Super-resolution with adaptive regularization. In *Proc. International Conf. on Image Processing (ICIP)*, volume 1, pages 169–172, 1997.
- [95] Sina Lotfian and Hassan Foroosh. View-invariant object recognition using homography constraints. In *Proc. IEEE International Conference on Image Processing (ICIP)*, 2017.
- [96] Fei Lu, Xiaochun Cao, Yuping Shen, and Hassan Foroosh. Camera calibration from two shadow trajectories. In *Proc. of IEEE International Conference on Advanced Video and Signal-based Surveillance*, volume 2.
- [97] Brian Millikan, Aritra Dutta, Qiyu Sun, and Hassan Foroosh. Compressed infrared target detection using stochastically trained least squares. *IEEE Transactions on Aerospace and Electronics Systems*, page accepted, 2017.
- [98] Brian Millikan, Aritra Dutta, Nazanin Rahnavard, Qiyu Sun, and Hassan Foroosh. Initialized iterative reweighted least squares for automatic target recognition. In *Military Communications Conference, MILCOM, IEEE*, pages 506–510, 2015.
- [99] Brian A. Millikan, Aritra Dutta, Nazanin Rahnavard, Qiyu Sun, and Hassan Foroosh. Initialized iterative reweighted least squares for automatic target recognition. In *Proc. of MILCOM*, 2015.
- [100] Brendan Moore, Marshall Tappen, and Hassan Foroosh. Learning face appearance under different lighting conditions. In *Proc. IEEE Int. Conf. on Biometrics: Theory, Applications and Systems*, pages 1–8, 2008.
- [101] Dustin Morley and Hassan Foroosh. Improving ransac-based segmentation through cnn encapsulation. In *Proc. IEEE Conf. on Computer Vision and Pattern Recognition (CVPR)*, 2017.
- [102] Pierre Poulin and John Amanatides. Shading and shadowing with linear light sources. *Computers and Graphics*, 15(2):259–265, 1991.
- [103] Ravi Ramamoorthi and Pat Hanrahan. An efficient representation for irradiance environment maps. In *SIGGRAPH '01: Proceedings of the 28th annual conference on Computer graphics and interactive techniques*, pages 497–500, New York, NY, USA, 2001. ACM Press.
- [104] H Shekarforoush. *Super-Resolution in Computer Vision*. PhD thesis, PhD Thesis, University of Nice, 1996.
- [105] H Shekarforoush, M Berthod, and J Zerubia. Sub-pixel reconstruction of a variable albedo lambertian surface. In *Proceedings of the British Machine Vision Conference (BMVC)*, volume 1, pages 307–316.
- [106] H Shekarforoush and R Chellappa. adaptive super-resolution for predator video sequences.
- [107] H Shekarforoush and R Chellappa. A multifractal formalism for stabilization and activity detection in flir sequences. In *Proceedings, ARL Federated Laboratory 4th Annual Symposium*, pages 305–309, 2000.
- [108] H Shekarforoush, R Chellappa, H Niemann, H Seidel, and B Girod. Multi-channel superresolution for images sequences with applications to airborne video data. *Proc. of IEEE Image and Multidimensional Digital Signal Processing*, pages 207–210, 1998.
- [109] Hassan Shekarforoush. *Conditioning bounds for multi-frame super-resolution algorithms*. Computer Vision Laboratory, Center for Automation Research, University of Maryland, 1999.
- [110] Hassan Shekarforoush. Noise suppression by removing singularities. *IEEE Trans. Signal Processing*, 48(7):2175–2179, 2000.
- [111] Hassan Shekarforoush. Noise suppression by removing singularities. *IEEE transactions on signal processing*, 48(7):2175–2179, 2000.
- [112] Hassan Shekarforoush, Amit Banerjee, and Rama Chellappa. Super resolution for fopen sar data. In *Proc. AeroSense*, pages 123–129. International Society for Optics and Photonics, 1999.
- [113] Hassan Shekarforoush, Marc Berthod, Michael Werman, and Josiane Zerubia. Subpixel bayesian estimation of albedo and height. *International Journal of Computer Vision*, 19(3):289–300, 1996.
- [114] Hassan Shekarforoush, Marc Berthod, and Josiane Zerubia. 3d super-resolution using generalized sampling expansion. In *Proc. International Conf. on Image Processing (ICIP)*, volume 2, pages 300–303, 1995.
- [115] Hassan Shekarforoush, Marc Berthod, and Josiane Zerubia. *Subpixel image registration by estimating the polyphase decomposition of the cross power spectrum*. PhD thesis, INRIA-Technical Report, 1995.
- [116] Hassan Shekarforoush, Marc Berthod, and Josiane Zerubia. Subpixel image registration by estimating the polyphase decomposition of cross power spectrum. In *Proc. IEEE Conf. Computer Vision and Pattern Recognition (CVPR)*, pages 532–537, 1996.
- [117] Hassan Shekarforoush and Rama Chellappa. Blind estimation of psf for out of focus video data. In *Image Processing, 1998. ICIP 98. Proceedings. 1998 International Conference on*, pages 742–745, 1998.
- [118] Hassan Shekarforoush and Rama Chellappa. Data-driven multi-channel super-resolution with application to video sequences. *Journal of Optical Society of America-A*, 16(3):481–492, 1999.
- [119] Hassan Shekarforoush and Rama Chellappa. A multi-fractal formalism for stabilization, object detection and tracking in flir sequences. In *Proc. of International Conference on Image Processing (ICIP)*, volume 3, pages 78–81, 2000.
- [120] Hassan Shekarforoush, Josiane Zerubia, and Marc Berthod. Denoising by extracting fractional order singularities. In *Proc. of IEEE International Conf. on Acoustics, Speech and Signal Processing (ICASSP)*, volume 5, pages 2889–2892, 1998.

- [121] Yuping Shen, Nazim Ashraf, and Hassan Foroosh. Action recognition based on homography constraints. In *Proc. of IAPR Int. Conf. Pattern Recognition (ICPR)*, pages 1–4, 2008.
- [122] Yuping Shen and Hassan Foroosh. View-invariant action recognition using fundamental ratios. In *Proc. IEEE Conference on Computer Vision and Pattern Recognition (CVPR)*, pages 1–6, 2008.
- [123] Yuping Shen and Hassan Foroosh. View invariant action recognition using fundamental ratios. In *Proc. IEEE Conference on Computer Vision and Pattern Recognition (CVPR)*, 2008.
- [124] Yuping Shen and Hassan Foroosh. View-invariant recognition of body pose from space-time templates. In *Proc. of IEEE Conf. on Computer Vision and Pattern Recognition*, pages 1–6, 2008.
- [125] Yuping Shen and Hassan Foroosh. View invariant recognition of body pose from space-time templates. In *Proc. IEEE Conference on Computer Vision and Pattern Recognition (CVPR)*, 2008.
- [126] Yuping Shen and Hassan Foroosh. View-invariant action recognition from point triplets. *IEEE Transactions on Pattern Analysis and Machine Intelligence (PAMI)*, 31(10):1898–1905, 2009.
- [127] Yuping Shen, Fei Lu, Xiaochun Cao, and Hassan Foroosh. Video completion for perspective camera under constrained motion. In *Proc. of IAPR Int. Conf. Pattern Recognition (ICPR)*, volume 3, pages 63–66, 2006.
- [128] Peter Shirley, Changyaw Wang, and Kurt Zimmerman. Monte carlo techniques for direct lighting calculations. *ACM Trans. Graph.*, 15(1):1–36, 1996.
- [129] Chen Shu, Luming Liang, Wenzhang Liang, and Hassan Foroosh. 3d pose tracking with multitemplate warping and sift correspondences. *IEEE Trans. on Circuits and Systems for Video Technology*, 26(11):2043–2055, 2016.
- [130] Michael M. Stark, William Martin, Elaine Cohen, Tom Lyche, and Richard F. Riesenfeld. B-splines for physically-based rendering.
- [131] Bo Sun, Ravi Ramamoorthi, Srinivasa G Narasimhan, and Shree K Nayar. A practical analytic single scattering model for real-time rendering. *ACM Transactions on Graphics (SIGGRAPH)*, August 2005.
- [132] Chuan Sun and Hassan Foroosh. Should we discard sparse or incomplete videos? In *Proceedings of IEEE International Conference on Image Processing (ICIP)*, pages 2502–2506, 2014.
- [133] Chuan Sun, Imran Junejo, and Hassan Foroosh. Action recognition using rank-1 approximation of joint self-similarity volume. In *Proc. IEEE International Conference on Computer Vision (ICCV)*, pages 1007–1012, 2011.
- [134] Chuan Sun, Imran Junejo, and Hassan Foroosh. Motion retrieval using low-rank subspace decomposition of motion volume. In *Computer Graphics Forum*, volume 30, pages 1953–1962. Wiley, 2011.
- [135] Chuan Sun, Imran Junejo, and Hassan Foroosh. Motion sequence volume based retrieval for 3d captured data. *Computer Graphics Forum*, 30(7):1953–1962, 2012.
- [136] Chuan Sun, Imran Junejo, Marshall Tappen, and Hassan Foroosh. Exploring sparseness and self-similarity for action recognition. *IEEE Transactions on Image Processing*, 24(8):2488–2501, 2015.
- [137] Chuan Sun, Marshall Tappen, and Hassan Foroosh. Feature-independent action spotting without human localization, segmentation or frame-wise tracking. In *Proc. of IEEE Conference on Computer Vision and Pattern Recognition (CVPR)*, pages 2689–2696, 2014.
- [138] T. Tanaka and T. Takahashi. Fast analytic shading and shadowing for area light sources. *Computer Graphics Forum*, 16(3), 1997.
- [139] Amara Tariq and Hassan Foroosh. Scene-based automatic image annotation. In *Proc. of IEEE International Conference on Image Processing (ICIP)*, pages 3047–3051, 2014.
- [140] Amara Tariq and Hassan Foroosh. Feature-independent context estimation for automatic image annotation. In *Proceedings of the IEEE Conference on Computer Vision and Pattern Recognition (CVPR)*, pages 1958–1965, 2015.
- [141] Amara Tariq, Asim Karim, and Hassan Foroosh. A context-driven extractive framework for generating realistic image descriptions. *IEEE Transactions on Image Processing*, 26(2):619–632, 2002.
- [142] Amara Tariq, Asim Karim, and Hassan Foroosh. Nelasso: Building named entity relationship networks using sparse structured learning. *IEEE Trans. on Pattern Analysis and Machine Intelligence*, 2017.
- [143] Amara Tariq, Asim Karim, Fernando Gomez, and Hassan Foroosh. Exploiting topical perceptions over multi-lingual text for hashtag suggestion on twitter. In *The Twenty-Sixth International FLAIRS Conference*, 2013.
- [144] Jiangjian Xiao, Xiaochun Cao, and Hassan Foroosh. 3d object transfer between non-overlapping videos. In *Proc. of IEEE Virtual Reality Conference*, pages 127–134, 2006.
- [145] Jiangjian Xiao, Xiaochun Cao, and Hassan Foroosh. A new framework for video cut and paste. In *Proc. of Int. Conf. on Multi-Media Modelling Conference Proceedings*, pages 8–pp, 2006.
- [146] Changqing Zhang, Xiaochun Cao, and Hassan Foroosh. Constrained multi-view video face clustering. *IEEE Transactions on Image Processing*, 24(11):4381–4393, 2015.